Equivalence of velocity statistics at constant pressure or constant altitude

R. G. Frehlich[1] and R. D. Sharman[2]

Received 13 February 2010; revised 10 March 2010; accepted 22 March 2010; published 17 April 2010.

[1] The equivalence of spatial velocity statistics calculated from second-order structure functions on constant pressure or constant altitude surfaces is demonstrated from analysis of numerical weather prediction model output, rawinsonde data, and commercial aircraft wind measurements. These large data sets allow the development of very accurate statistics. Turbulence scaling laws for horizontal velocity statistics are found to be equivalent for either calculation. **Citation:** Frehlich, R. G., and R. D. Sharman (2010), Equivalence of velocity statistics at constant pressure or constant altitude, *Geophys. Res. Lett.*, *37*, L08801, doi:10.1029/2010GL042912.

1. Introduction

[2] Spatial velocity statistics (spatial spectra, structure functions, or covariance functions) describe the atmospheric dynamics as a function of spatial scale, season, and geographic region. Various spatial velocity statistics have been produced from the analysis of aircraft observations [*Nastrom and Gage*, 1985; *Lindborg*, 1999; *Frehlich and Sharman*, 2010], Numerical Weather Prediction (NWP) model output [*Skamarock*, 2004; *Frehlich and Sharman*, 2004, 2008], Global Climate Model (GCM) output [*Koshyk and Hamilton*, 2001; *Takahashi et al.*, 2006; *Hamilton et al.*, 2008], and rawinsonde observations [*Frehlich and Sharman*, 2010]. Spatial statistics have also been investigated using idealized numerical simulations [*Lindborg*, 2005, 2006; *Waite and Bartello*, 2006; *Waite and Snyder*, 2009]. However, all past results based on observations (aircraft and rawinsonde) have been calculated on constant pressure levels, and *Lovejoy et al.* [2009, 2010] have indicated that these statistics should be performed on constant altitude levels because of the large altitude variations of the pressure surfaces associated with synoptic scale disturbances. They also propose that the turbulence scaling laws are different for constant pressure levels and constant altitude levels. This interpretation has been challenged by *Lindborg et al.* [2009]. Further, *Skamarock* [2004] found that spatial velocity spectra from NWP model output were equivalent for calculations on constant pressure or constant altitude levels. Here, results are presented from second-order structure function analyses of NWP model output, commercial aircraft data, and rawinsonde data that convincingly demonstrate the equivalence of spatial velocity statistics calculated on constant pressure and constant altitude levels when the data is taken over sufficiently long time periods (at least one year).

2. Observations

[3] For this study, the observations used are from the rawinsonde network and three sources of meteorological observations from commercial aircraft: the Aircraft Communications, Addressing, and Reporting System (ACARS), the Aircraft Meteorological Data Relay (AMDAR), and the Tropospheric Airborne Meteorological Data Reporting (TAMDAR) system [*Daniels et al.*, 2006; *Moninger et al.*, 2009]. The accuracy of the rawinsonde data is 0.5 m s^{-1} in each horizontal velocity component [*Jaatinen and Elms*, 2000] and altitude is calculated from the temperature and pressure profiles provided through the hydrostatic relation.

[4] For the ACARS and AMDAR observations, the accuracy of each horizontal wind component is approximately 1.25 – 1.5 m s^{-1} [*Benjamin et al.*, 1999; *Drüe et al.*, 2008]. As with aircraft data used by *Nastrom and Gage* [1985], *Lindborg* [1999], and others, the ACARS/AMDAR data reports altitude calculated from the pressure using the standard atmosphere and does not provide independent altitude information. However, the TAMDAR data does include pressure and GPS altitude and therefore permits the calculation of velocity statistics on both constant pressure and constant altitude levels over the Continental US (CONUS).

3. RUC NWP Model

[5] Statistical analysis is performed using NCEP's Rapid Update Cycle (RUC) model output [*Benjamin et al.*, 2004]. In principle, any NWP model could be used for this analysis, but the RUC model was chosen because of the fairly high horizontal resolution (grid spacing about 13 km), the higher effective vertical resolution provided by the isentropic vertical coordinate system at upper-levels in the model, and the lengthy archive available (2 years). This model is a hydrostatic model which ignores vertical accelerations and Coriolis terms in the vertical equation of motion. This is a very good approximation for the scales of motion resolved by the model as a simple scale analysis demonstrates [*Holton*, 2004, section 2.4.3].

4. Structure Function Analysis

[6] Structure functions are ideally suited for the calculation of spatial statistics with a non-uniform observation

[1]CIRES, University of Colorado at Boulder, Boulder, Colorado, USA.
[2]Research Applications Laboratory, National Center for Atmospheric Research, Boulder, Colorado, USA.

0094-8276/10/2010GL042912

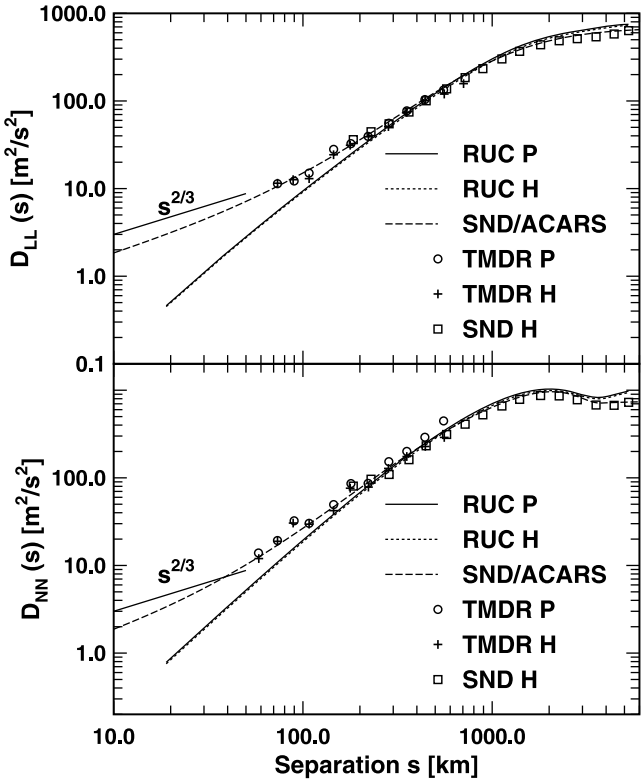

Figure 1. Spatial structure functions of the longitudinal velocity $D_{LL}(s)$ and transverse velocity $D_{NN}(s)$ as a function of separation s for a constant pressure level 250 hPa and constant altitude levels centered at 10.438 km. The results for constant pressure levels are the RUC model (RUC P), rawinsonde and ACARS/AMDAR data (SND/ACARS), and the TAMDAR data (TMDR P). The results for constant altitude levels are the RUC model (RUC H), rawinsonde (SND H), and the TAMDAR data (TMDR H). The rms altitude variations $H_{RMS} = 295$ m from the rawinsonde data on the 250 hPa level. The $s^{2/3}$ line at small separations is shown for comparison.

system [*Frehlich and Sharman*, 2010]. The structure function of variable u on a constant pressure level p is defined as

$$D_{uu}(s,p) = \langle [u(s_1,p,z_1) - u(s_1+s,p,z_2)]^2 \rangle \qquad (1)$$

where $\langle\ \rangle$ denotes an ensemble average, and $u(s, p, z)$ denotes the variable at horizontal location s, and altitude z. By substituting $u(s_1 + s, p_2, z_1) - u(s_1 + s, p_2, z_1) = 0$ into equation (1) and expanding gives

$$D_{uu}(s,p) = D_{uu}(s,\overline{z}) + D_{uu}(\overline{s_z},\overline{z}) + 2C_{uu}(s,\overline{s_z},\overline{p},\overline{z}) \qquad (2)$$

where $D_{uu}(s, \overline{z}) = \langle [u(s_1, p, z_1) - u(s_1 + s, p_2, z_1)]^2 \rangle$ is the structure function for constant altitude at the average altitude $\overline{z}$, $D_{uu}(\overline{s_z}, \overline{z}) = \langle [u(s_1 + s, p_2, z_1) - u(s_1 + s, p, z_2)]^2 \rangle$ is the structure function of u for the average vertical displacement $\overline{s_z} = \langle |z_2 - z_1| \rangle$ and $C_{uu}(s, \overline{s_z}, \overline{p}, \overline{z}) = \langle [u(s_1, p, z_1) - u(s_1 + s, p_2, z_1)][u(s_1 + s, p_2, z_1) - u(s_1 + s, p, z_2)] \rangle$. The equivalence of the structure functions on constant pressure $D_{uu}(s, p)$ and constant altitude $D_{uu}(s, \overline{z})$ therefore requires that the last two terms of equation (2) are negligible compared to the first term. Note that C_{uu} is approximately zero for typical horizontal mesoscale separations s since the two velocity differences are uncorrelated.

[7] Since there can be small variations in the velocity statistics with altitude and latitude [*Nastrom and Gage*, 1985; *Cho and Lindborg*, 2001; *Frehlich and Sharman*, 2010], here the structure functions were calculated for the latitude band 40–50 N over CONUS which has a relatively high density of ACARS and TAMDAR data [*Moninger et al.*, 2009], and is also in the middle of the RUC computational domain. The horizontal velocity vector was decomposed into a longitudinal component v_L and a transverse or normal component v_N based on the location of each data pair [*Frehlich and Sharman*, 2010]. The longitudinal D_{LL} and transverse or normal D_{NN} structure functions as a function of separation distance s then describe the second-order horizontal velocity statistics.

[8] Structure functions can be computed on constant pressure or constant altitude levels using rawinsonde, TAMDAR, and NWP data. Structure functions from the RUC NWP model were calculated on constant pressure surfaces and the constant altitude surface corresponding to the average altitude of each constant pressure surface. To improve the statistical accuracy of the structure function estimates when using the TAMDAR data, the data was first collected into small altitude layers (for constant altitude calculations) or into small pressure layers (for constant pressure calculations) before computing an average structure function from the multiple layers. For calculations on constant pressure levels, the bin interval was 4 hPa and 11 levels were averaged around the chosen reference pressure level. For calculations on constant altitude levels, the bin interval was 200 m and 5 intervals were averaged around the reference altitude for a total altitude interval of 1 km which is a good match to the range of average altitude from the constant pressure level estimates. If a random variable has a uniform distribution over an interval Δ, the rms or standard deviation is $\Delta/\sqrt{12}$ [*Parzen*, 1960]. Therefore, if the observations are uniformly distributed over the 200 m altitude interval, the rms altitude variations are $200/\sqrt{12} = 57.7$ m and the structure functions can be considered constant altitude estimates. Quality control checks of the aircraft observations were performed as described by *Frehlich and Sharman* [2010]. The structure function estimates were rejected if the total number of data pairs for either calculation (constant altitude or constant pressure) was less than 500.

[9] The time periods of the data used are: rawinsonde measurements 34 years from 1973 to 2006; ACARS/AMDAR observations 2001 to 2008; TAMDAR data 2009; and RUC model output for 2006 and 2007. Statistical accuracy improves with longer observation periods which produce more independent samples of the larger scale synoptic features. Therefore, the rawinsonde data produces the most accurate results, followed by ACARS/AMDAR, then the RUC model and finally the TAMDAR data.

[10] Results for the 250 hPa constant pressure level and the corresponding constant altitude calculations centered on 10.438 km (the average altitude of this pressure level) are shown in Figure 1. For this pressure level, the standard deviation of the rawinsonde altitude was 295 m compared to 57.7 m for the TAMDAR data. The constant pressure and constant altitude structure functions from the RUC model

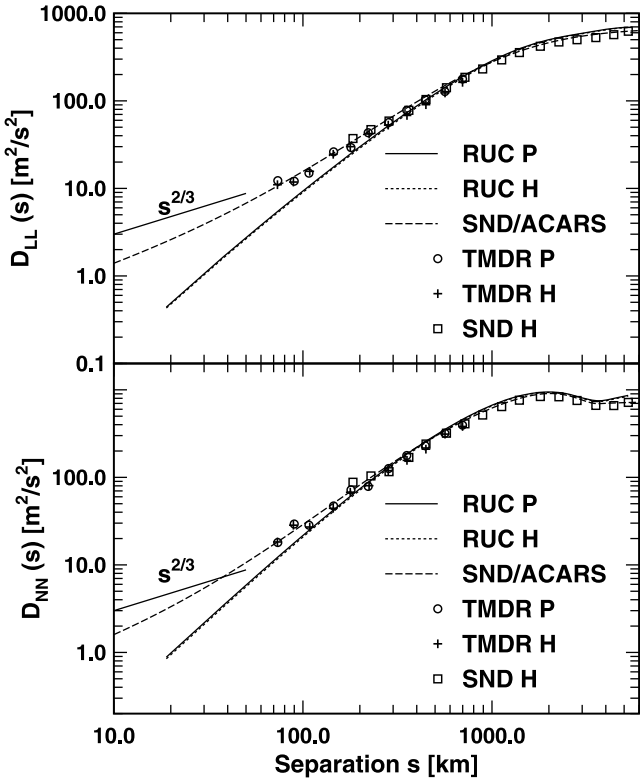

Figure 2. Same as Figure 1 except for a constant pressure level of 300 hPa and constant altitude levels centered at 9.232 km. The rms altitude variation is H_{RMS} = 276 m from the rawinsonde data.

agree to better than 5% over the full spatial separation domain of the calculations. There is also good agreement of the RUC constant pressure estimates with the ACARS/AMDAR estimates for spatial scales larger than 300 km where the effects of the spatial filtering by the numerics of the RUC model are negligible. The constant pressure and the constant altitude estimates derived from the TAMDAR data are in very good agreement, even though the statistical accuracy is less because of the smaller data set available. Also, the structure functions of the rawinsonde data interpolated to constant altitude are in good agreement with the empirical model for constant pressure derived from the ACARS/AMDAR and rawinsonde data at constant pressure levels [*Frehlich and Sharman*, 2010]. Similar results are produced for the 300 hPa pressure level as shown in Figure 2.

[11] The 500 hPa region in the middle troposphere shown in Figure 3 contains the largest amount of TAMDAR data and therefore provides the largest coverage of the spatial scales of interest. Again, there is good agreement among all structure function estimates. The increase in spectral slope at 250 hPa compared with 500 hPa is most likely a consequence of the energetic jet stream at 250 hPa which has a typical spacing of approximately 2000 km. This is demonstrated by the peak of the transverse structure function D_{NN} in Figures 1–3. Note that all the structure functions show a deviation from the $s^{2/3}$ scaling at intermediate to large scales.

[12] The most likely explanation for the equivalence between constant pressure and constant altitude statistics is that the contribution from the average vertical displacements $D_{uu}(\overline{s_z}, \overline{z})$ in equation (2) is small compared with the term $D_{uu}(s, \overline{z})$, as discussed by *Lindborg et al.* [2009]. Note that the average altitude difference $\overline{s_z}$ on constant pressure surfaces is on the order of the rms altitude variations H_{rms} of the constant pressure surface. Therefore $\overline{s_z}$ < 300 m (see captions of Figures 1–3). From Figure 1 of *Lovejoy et al.* [2007], the term $\sqrt{D_{uu}(\overline{s_z}, \overline{z})} < 1$ for $\overline{s_z}$ = 300 m and therefore $D_{uu}(s, p)$ and $D_{uu}(s, \overline{z})$ agree to better than 1% for a horizontal spacing of s = 1000 km since $D_{uu}(s, \overline{z}) > 100$ (see Figures 1–3) and $C_{uu}(s, \overline{s_z}, \overline{p}, \overline{z}) \approx 0$.

[13] Regarding the spectral slope, the structure functions estimates can be related to spatial spectra by simple empirical models, e.g., [*Hinze*, 1959]

$$D(s) = 2\sigma_{VK}^2\left[1 - \frac{2^{2/3}}{\Gamma(1/3)}\left(\frac{s}{L_{VK}}\right)^{1/3} K_{1/3}\left(\frac{s}{L_{VK}}\right)\right] + 2\sigma_{LS}^2\left[1 - \frac{2^{1-\nu}}{\Gamma(\nu)}\left(\frac{s}{L_{LS}}\right)^{\nu} K_{\nu}\left(\frac{s}{L_{LS}}\right)\right] \quad (3)$$

where $K_\nu(z)$ is the modified Bessel function of order ν, σ_{VK} and σ_{LS}, and L_{VK} and L_{LS}, are the standard deviation and outer length scale of the von-Kármán and large scale component, respectively. The corresponding one-dimensional spectrum from equation (3) is [*Hinze*, 1959]

$$E(k) = \frac{\Gamma(5/6)\sigma_{VK}^2 L_{VK}}{\Gamma(1/3)\sqrt{\pi}\left(1 + L_{VK}^2 k^2\right)^{5/6}} + \frac{\Gamma(\nu + 1/2)\sigma_{LS}^2 L_{LS}}{\Gamma(\nu)\sqrt{\pi}\left(1 + L_{LS}^2 k^2\right)^{\nu+1/2}} \quad (4)$$

which consists of two power-law components with a scaling of $k^{-5/3}$ at high wavenumbers k and $k^{-2\nu-1} = k^{-\beta}$ at low wavenumbers where $\beta = 2\nu + 1$. A best-fit of equation (3) to all the ACARS/SND structure functions in Figures 1–3 for separations <1000 km produces the following estimates of the slope β: 3.08, 2.77, and 2.65 for the longitudinal component and 3.36, 3.05, and 2.88 for the transverse component at 250, 300, and 500 hPa, respectively. Note that this procedure produces quantitative estimates of the spectral slopes without the need for a subjective choice of a region for fitting a straight line. We therefore conclude that these results are consistent with past estimates of a low wavenumber spectral slope of −3 which are based on average spectra over different altitude and latitude ranges. However, there is typically only a decade of approximate power-law scaling at low wavenumbers and there are clear variations of the slope with altitude, latitude, season, and geographical regions [*Nastrom and Gage*, 1985; *Lindborg*, 1999; *Cho and Lindborg*, 2001; *Frehlich and Sharman*, 2010], so assigning a single universal value to the slope is not appropriate.

[14] In any event, based on theoretical considerations, *Lovejoy et al.* [2009, 2010] argue that the spectral slope at low wavenumbers should obey a $k^{-2.4}$ scaling instead of the k^{-3} scaling found in previous aircraft observational studies of *Nastrom and Gage* [1985], *Lindborg* [1999], and others. They maintain this discrepancy is due in part to the fact that the observations were taken on constant pressure surfaces rather than on constant altitude surfaces. However, in agreement with *Skamarock* [2004], our structure function analysis of two independent sources of observations (rawinsonde and TAMDAR), and of NWP derived data, all indicate that there is no significance difference between the

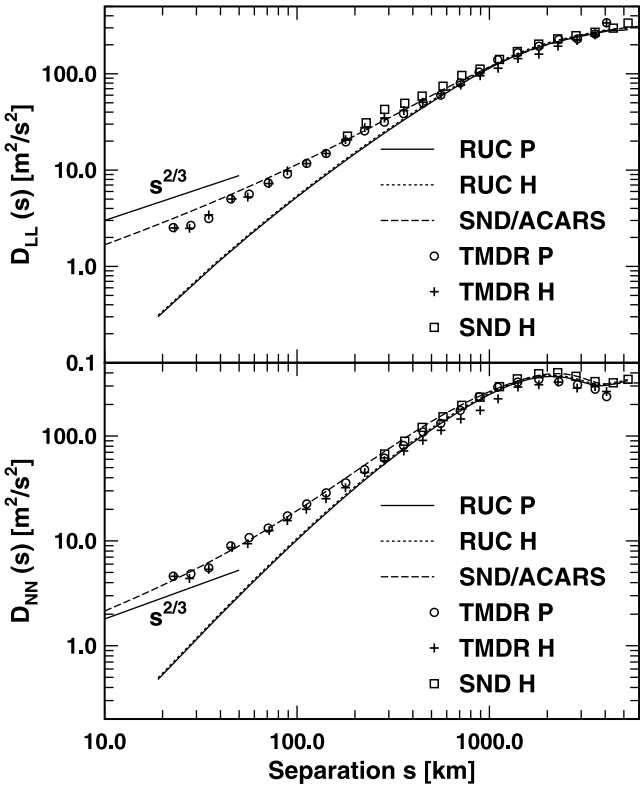

Figure 3. Same as Figure 1 except for a constant pressure level of 500 hPa and constant altitude levels centered at 5.614 km. The rms altitude variation is H_{RMS} = 181 m from the rawinsonde data.

spatial statistics computed on constant pressure surfaces and those computed at nearly the same level but on constant altitude surfaces.

5. Summary and Discussion

[15] The equivalence of spatial velocity statistics derived from second-order structure functions calculated on constant pressure or constant altitude surfaces was demonstrated by comparisons of estimates from NWP model output and aircraft observations. These results are consistent with the claim of *Skamarock* [2004], viz., "We have also computed spectra on constant pressure surfaces and on constant height surfaces and found that there is little significant difference among these spectra." The most likely explanation for this equivalence is that for constant pressure levels in extra-tropical regions, the variations in horizontal velocity differences at large separations (on the order of 1000 km) due to altitude changes interacting with the vertical wind shear are small compared with the magnitude of the horizontal velocity differences at constant altitude, as discussed by *Lindborg et al.* [2009].

[16] The deviations of the $s^{2/3}$ scaling at small separations s to a steeper scaling at larger separations is a very robust result but has a latitude and altitude dependence which has implications for the theoretical predictions of atmospheric turbulence. However, there is only about a decade of the steeper power-law scaling before the structure functions flatten out at the largest scales. This makes it difficult to accurately fit a power-law (structure function or spectra) to this region. Further, the slope of the fit is regionally and seasonally dependent. Thus, a single universal scaling exponent is unlikely to be found.

[17] Quantitative error analysis is difficult because of the different spatial sampling of the data and the different temporal correlations in the atmospheric processes. However, as more data becomes available, robust statistical analysis can be produced with yearly-averaged estimates.

[18] **Acknowledgments.** This work was funded in part by NSF grants ATM0646401 and ATM0522004 and by grants from the NASA ASAP program. We appreciate the very helpful comments of Bill Skamarock and Erik Lindborg.

References

Benjamin, S. G., B. E. Schwartz, and R. E. Cole (1999), Accuracy of ACARS wind and temperature observations determined by collocation, *Weather Forecast.*, *14*, 1032–1038.

Benjamin, S. G., G. A. Grell, J. M. Brown, and T. G. Smirnova (2004), Mesoscale weather prediction with the RUC hybrid isentropic-terrain-following coordinate model, *Mon. Weather Rev.*, *132*, 473–494.

Cho, J. Y. N., and E. Lindborg (2001), Horizontal velocity structure functions in the upper troposphere and lower stratosphere: 1. Observations, *J. Geophys. Res.*, *106*, 10223–10232, doi:10.1029/2000JD900815.

Daniels, T. S., W. R. Moninger, and R. D. Mamrosh (2006), Tropospheric Airborne Meteorological Data Reporting (TAMDAR) Overview, paper presented at 12th Conference on Aviation, Range, and Aerospace Meteorology (ARAM), Am. Meteorol. Soc., Atlanta.

Drüe, C., W. Frey, A. Hoff, and Th. Hauf (2008), Aircraft type-specific errors in AMDAR weather reports from commercial aircraft, *Q. J. R. Meteorol. Soc.*, *134*, 229–239.

Frehlich, R., and R. Sharman (2004), Estimates of turbulence from numerical weather prediction model output with application to turbulence diagnosis and data assimilation, *Mon. Weather Rev.*, *132*, 2308–2324.

Frehlich, R., and R. Sharman (2008), The use of structure functions and spectra from numerical model output to determine effective model resolution, *Mon. Weather Rev.*, *136*, 1537–1553.

Frehlich, R., and R. Sharman (2010), Climatology of velocity and temperature turbulence statistics determined from rawinsonde and ACARS/AMDAR data, *J. Appl. Meterolol. Clim.*, in press.

Hamilton, K., Y. O. Takahashi, and W. Ohfuchi (2008), Mesoscale spectrum of atmospheric motions investigated in a very fine resolution global general circulation model, *J. Geophys. Res.*, *113*, D18110, doi:10.1029/2008JD009785.

Hinze, J. O. (1959), *Turbulence: An Introduction to Its Mechanism and Theory*, 586 pp., McGraw-Hill, New York.

Holton, J. R. (2004), *An Introduction to Dynamic Meteorology*, 4th ed., 535 pp., Academic, New York.

Jaatinen, J., and J. B. Elms (2000), On the windfinding accuracy of Loran-C, GPS and radar, *Väisälä News*, *152*, 30–33.

Koshyk, J. N., and K. Hamilton (2001), The horizontal kinetic energy spectrum and spectral budget simulated by a high-resolution troposphere-stratosphere-mesosphere GCM, *J. Atmos. Sci.*, *58*, 329–348.

Lindborg, E. (1999), Can the atmospheric kinetic energy spectrum be explained by two-dimensional turbulence?, *J. Fluid Mech.*, *388*, 259–288.

Lindborg, E. (2005), The effect of rotation on the mesoscale energy cascade in the free atmosphere, *Geophys. Res. Lett.*, *32*, L01809, doi:10.1029/2004GL021319.

Lindborg, E. (2006), The energy cascade in a strongly stratified fluid. *J. Fluid Mech.*, *550*, 207–242.

Lindborg, E., K. K. Tung, G. D. Nastrom, J. Y. N. Cho, and K. S. Gage (2009), Comment on "Reinterpreting aircraft measurements in anisotropic scaling turbulence" by Lovejoy et al. (2009), *Atmos. Chem. Phys. Discuss.*, *9*, 22,331–22,336.

Lovejoy, S., A. F. Tuck, S. J. Hovde, and D. Schertzer (2007), Is isotropic turbulence relevant in the atmosphere?, *Geophys. Res. Lett.*, *34*, L15802, doi:10.1029/2007GL029359.

Lovejoy, S., A. F. Tuck, D. Schertzer, and S. J. Hovde (2009), Reinterpreting aircraft measurements in anisotropic scaling turbulence, *Atmos. Chem. Phys.*, *9*, 5007–5025.

Lovejoy, S., A. F. Tuck, and D. Schertzer (2010), The horizontal cascade structure of atmospheric fields determined from aircraft data, *J. Geophys. Res.*, doi:10.1029/2009JD013353, in press.

Moninger, W. R., S. G. Benjamin, B. D. Jamison, T. W. Schlatter, T. L. Smith, and E. J. Szoke (2009), TAMDAR jet fleets and their impact on

rapid update cycle (RUC) forecasts, paper presented at 13th Conference on Integrated Observing and Assimilation Systems for Atmospheres, Oceans, and Land Surface, Am. Meteorol. Soc., Phoenix, 29 Jan.

Nastrom, G. D., and K. S. Gage (1985), A climatology at atmospheric wavenumber spectra of wind and temperature observed by commercial aircraft, *J. Atmos. Sci.*, *42*, 950–960.

Parzen, E. (1960), *Modern Probability Theory and Its Applications*, 464 pp., John Wiley, Oxford, U. K.

Skamarock, W. C. (2004), Evaluating mesoscale NWP models using kinetic energy spectra, *Mon. Weather Rev.*, *132*, 3019–3032.

Takahashi, Y. O., K. Hamilton, and W. Ohfuchi (2006), Explicit global simulation of mesoscale spectrum of atmospheric motions, *Geophys. Res. Lett.*, *33*, L12812, doi:10.1029/2006GL026429.

Waite, M. L., and P. Bartello (2006), The transition from geostrophic to stratified turbulence, *J. Fluid Mech.*, *568*, 89–108.

Waite, M. L., and C. Snyder (2009), The mesoscale kinetic energy spectrum of a baroclinic life cycle, *J. Atmos. Sci.*, *66*, 883–901.

R. G. Frehlich, CIRES, UCB 215, University of Colorado at Boulder, Boulder, CO 80309, USA. (Rodney.Frehlich@Colorado.edu)

R. D. Sharman, Research Applications Laboratory, National Center for Atmospheric Research, Boulder, CO 80305, USA. (sharman@ucar.edu)